In proc. *ROMANSY 18 - Robot Design, Dynamics and Control*, July 5-8, 2010, Udine, Italy, pp. 331-338.

Motion Control of an Under-Actuated Service Robot Using Natural Coordinates

László L. Kovács [*‡], Ambrus Zelei [‡], László Bencsik [‡], János Turi [†] and Gábor Stépán [‡]

[*] HAS-BME Research Group on Dynamics of Machines and Vehicles
[†] The University of Texas at Dallas, Department of Mathematical Sciences
[‡] Budapest University of Technology and Economics, Department of Applied Mechanics

Abstract The recent work presents the motion control of a pendulum like under–actuated service robot ACROBOTER. This robot is designed to be applied in indoor environments, where it can perform pick and place tasks autonomously and/or with close cooperation with humans. It can also serve as a platform that carries other service robots with lower mobility. The cable suspended robot has a complex structure and its dynamics is difficult to model using conventional robotic approaches. Instead, in this paper natural (Cartesian) coordinates are used to describe the configuration of the robot, while its dynamics is modeled as a set of differential algebraic equations. The method of computed torque control with a PD controller is applied to the investigated under–actuated system. The inverse dynamics solution is obtained via direct discretization of the DAE system. Results for a real parameter case study are presented by numerical simulations.

1 Introduction

Obstacle avoidance is an important problem in service and mobile robotics, especially when the robots are operating in an everyday indoor environment. Static obstacles on the floor of a room include various objects such as stairs, doorsteps, chairs, tables and even the edges of carpets. Hence,

This work was supported in part by the Hungarian National Science Foundation under grant no. OTKA K068910, the ACROBOTER (IST-2006-045530) project, the Hungarian Academy of Sciences under grant no. MTA-NSF/103, the HAS-BME Research Group on Dynamics of Machines and Vehicles and by National Science Foundation DMS-0705247.

floor based domestic robots need to have strategies to overcome randomly placed objects.

A new direction in the development of indoor service robots is the use of robotic structures that can move on the, almost obstacle free, ceiling of a room. An application which addresses the need for a robot to climb on the walls and crawl on the ceiling inside a building is the MATS robot (Balaguer et al., 2006). Another examples include actuator mechanisms showing similarities with gantry cranes, e.g., the mobile robot platform described in (Sato et al., 2004) and the FLORA walking assisting system developed by FATEC Corporation (FATEC Co., 2004). These platform concepts solve the problem of avoiding obstacles on the floor, while they are able to roam over almost the whole inner space of a room, and compared to gantry cranes, they enable the use of co-operating multiple units.

The present paper describes a new indoor service robot platform developed within the ACROBOTER IST-2006-045530 project (Stépán and et al, 2009). The ceiling suspended robot (see Figure 1a) is equipped with windable cables and ducted fan actuators. Compared to (Sato et al., 2004; FATEC Co., 2004) the use of complementary actuators makes it possible to control and utilize the pendulum-like motion of the system, and provide larger workspace and better maneuverability. The ACROBOTER robot is able to move along a prescribed spatial trajectory while it performs various tasks like pick and place of objects and manipulating other service robots. Despite of the large number of actuators, the ACROBOTER robot is still under–actuated. The application of the method of computed torque control for this system leads to a set of differential algebraic equations adjoining to the geometric constraints which also appear as algebraic equations. The generalized coordinates that describe the configuration of the system are coupled and cannot be partitioned into passive and active coordinates in general. Instead, in this paper the direct solution of the DAE problem is presented for ACROBOTER system using the Backward-Euler discretization method as it is also proposed in (Blajer and Kolodziejczyk, 2008). The algorithm is formulated semi-analitically. Its applicability is demonstrated by numerical experiments.

2 Mechanical Model and Problem Formulation

The ACROBOTER system shown in Figure 1a consists of Anchor Points (AP) placed on the ceiling, a Climer Unit (CU) that can swap between these APs and a Swinging Unit (SU) which has a mechanical interface for connecting the payload. The CU is an RRT robot that moves parallel to the ceiling and provides the horizontal motion of the system. The windable

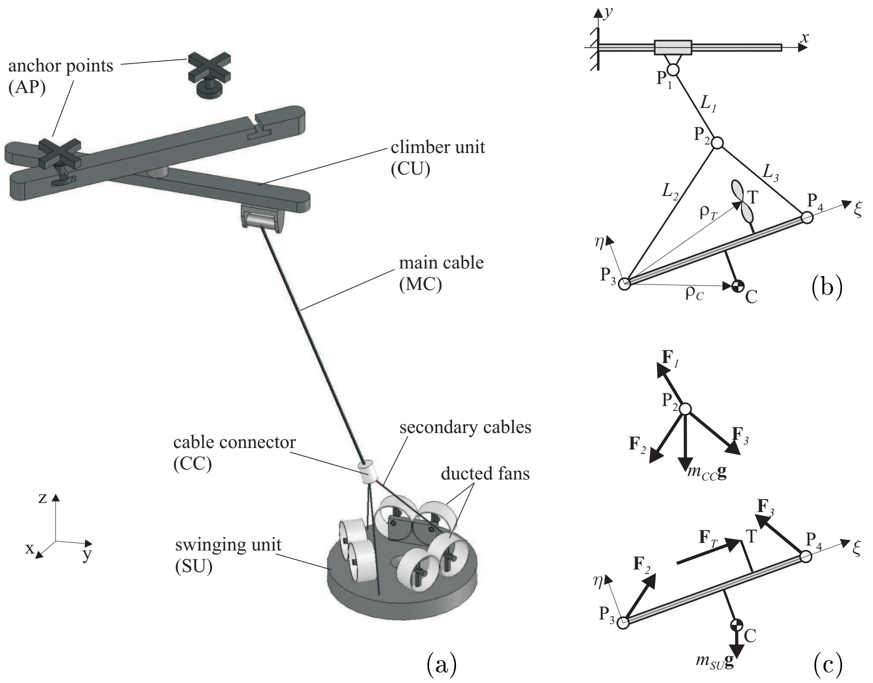

Figure 1. ACROBOTER (a), planar model (b), free body diagrams (c)

Main Cable (MC) connects the CU and the SU through the Cable Connector (CC) to which the secondary orienting cables are also attached. By using the mechanical interface the Swinging Unit (SU) can be equipped with grippers and various tools. In this concept the three secondary cables orient the SU, while the three pairs of ducted fans are used for performing and stabilizing the motion of the SU along its desired trajectory. The thrust forces provided by the ducted fans make it possible to move the payload even when the CU does not move at all.

For developing the control algorithm of this device we consider the planar model of the ACROBOTER (see Figure 1b). The free-body-diagrams corresponding to this model are shown in Figure 1c. We treat the robot as a multibody system described by natural (Cartesian) coordinates (de Jalón and Bayo, 1994). This formalism provides the equation of motion for both the planar and spatial cases in the same form. Modeling of the spatial ACROBOTER system does not require further complexity, only the number of descriptor coordinates and geometric constraints will be higher.

In Figure 1b the SU is modeled as a rod with length L_{34} and mass m_{SU}, which includes the mass of the payload as well. The CC is considered as a point mass m_{CC}. The length of the MC is denoted by L_1 and the corresponding cable force is $\mathbf{F}_1$. The actuator forces acting upon the secondary cables are $\mathbf{F}_2$ and $\mathbf{F}_3$, respectively. The configuration of the system is described by the coordinates (x_i, z_i) of the points P_i. In addition, the center of mass of the SU is given by the vector $\boldsymbol{\rho}_C$ in the body frame, and the loading point of the resultant thrust force is represented by the vector $\boldsymbol{\rho}_T$.

By considering that the CU moves exactly on a prescribed trajectory and using the set of descriptor coordinates $\mathbf{q} = [x_2, z_2, x_3, z_3, x_4, z_4]^{\mathrm{T}}$, the equation of motion of the ACROBOTER system can be written as

$$\mathbf{M}\ddot{\mathbf{q}} + \boldsymbol{\Phi}_{\mathbf{q}}^{\mathrm{T}}(\mathbf{q})\boldsymbol{\lambda} = \mathbf{Q}_g + \mathbf{H}(\mathbf{q})\mathbf{u} \,, \tag{1}$$

$$\boldsymbol{\phi}(\mathbf{q}) = \mathbf{0} \,, \tag{2}$$

$$\boldsymbol{\phi}_s(\mathbf{q}, \mathbf{p}(t)) = \mathbf{0} \,. \tag{3}$$

Equation (1) is a Lagrangian equation of motion of the first kind, where $\mathbf{M}$ is the $n \times n$ sized constant mass matrix (de Jalón and Bayo, 1994) which may also depend on the payload. Symbol $\mathbf{Q}_g$ is the generalized gravity force. The m geometric constraints are represented by the vector $\boldsymbol{\phi}(\mathbf{q})$ in (2) and $\boldsymbol{\Phi}_{\mathbf{q}}$ is the Jacobian matrix of the constraints. The corresponding Lagrange multipliers are denoted by $\boldsymbol{\lambda}$. The l dimension input vector is $\mathbf{u}$ and $\mathbf{H}$ is the generalized input matrix.

The number of control inputs, l, is less than the $n - m$ DoFs of the system, thus it is under-actuated. The task of the robot can be formulated by the servo-constraints $\boldsymbol{\phi}_s(\mathbf{q}, \mathbf{p}(t))$ (Blajer and Kolodziejczyk, 2008) given in equation (3). The dimension of the $\boldsymbol{\phi}_s(\mathbf{q}, \mathbf{p}(t))$ vector is also l which means that the l dimensional control input can be determined uniquely.

The servo constraints depend on the function $\mathbf{p}(t)$ that can be handled as the desired system output and it may describe the desired trajectory of a certain point and/or the desired orientation of the SU. For example, if the position of the center of mass of the SU and its horizontal orientation is prescribed together with the elevation of the CC, the servo constraints can be expressed in the form

$$\boldsymbol{\phi}_s(\mathbf{q}, \mathbf{p}(t)) = \mathbf{h}(\mathbf{q}) - \mathbf{p}(t) \quad \text{with} \tag{4}$$

$$\mathbf{h}(\mathbf{q}) = [1/2(x_3 + x_4),\, 1/2(y_3 + y_4),\, y_3 - y_4,\, y_2]^{\mathrm{T}} \,, \tag{5}$$

$$\mathbf{p}(t) = \left[x_C^d(t),\, y_C^d(t),\, 0,\, y_2^d(t)\right]^{\mathrm{T}} \,, \tag{6}$$

where $\mathbf{h}(\mathbf{q})$ gives the prescribed system outputs as the function of the descriptor coordinates by assuming that $\boldsymbol{\rho}_C = [L_{34}/2,\, 0]^{\mathrm{T}}$.

We assume that the servo-constraints and a well chosen subset of geometric constraints can be solved for the controlled coordinates $\mathbf{q}_c$ in closed form.

Then the task can be defined by $\mathbf{q}_c = \mathbf{q}_c^d$, where the superscript d refers to the desired trajectory. In the case of the planar ACROBOTER model the vector of these desired coordinates is $\mathbf{q}_c^d = [y_2^d(t),\, x_3^d(t),\, y_3^d(t),\, y_4^d(t)]^{\mathrm{T}}$. For the partitioning of the descriptor coordinates we introduce the vector of controlled and uncontrolled coordinates with $\mathbf{q}_c = \mathbf{S}_c^{\mathrm{T}}\mathbf{q}$ and $\mathbf{q}_u = \mathbf{S}_u^{\mathrm{T}}\mathbf{q}$, respectively, where $\mathbf{S}_c$ and $\mathbf{S}_u$ are task dependent selector matrices.

3 Computed Torque Control

The computed torque method was generalized in (Lammerts, 1993) for the case of under-actuated systems. The generalized method is called Computed Desired Computed Torque Control method (CDCTC), where the expression "computed desired" refers to the fact that the uncontrolled coordinates cannot be prescribed arbitrarily, since they depend on the internal dynamics of the system. In case of the CDCTC method the equations of motion are ordinary differential equations (ODE) and the null space of the coefficient matrix of the input vector is used to project these equations into the space of uncontrolled motions. The projected set of differential equations can then be solved for the desired values of the uncontrolled coordinates and the control inputs can then be expressed.

To apply the CDCTC method to the ACROBOTER model described by equations (1–3) an additional projection is required. Since the equations of motion are given as a DAE system, first, the DAE system has to be reduced to an ODE. This can be accomplished by projecting the equations of motion to the subspace of admissible motions by the constraints (Kövecses et al., 2003). However, the repeated projections and the stabilization (configuration correction) of the numerical solution make the application of the method rather complex and computationally expensive.

Instead, we apply the Backward Euler discretization for the DAE system and the resulting set of implicit equations are solved by the Newton-Raphson method for the desired actuator forces. Considering a PD controller with gain matrices $\mathbf{K}_P$ and $\mathbf{K}_D$ the control law can be formulated as

$$\mathbf{M}\ddot{\mathbf{q}}^d + \boldsymbol{\Phi}_{\mathbf{q}}^{\mathrm{T}}(\mathbf{q}^d)\boldsymbol{\lambda} = \mathbf{Q}_g + \mathbf{H}(\mathbf{q}^d)\mathbf{u} - \mathbf{K}_P(\mathbf{q}^d - \mathbf{q}) - \mathbf{K}_D(\dot{\mathbf{q}}^d - \dot{\mathbf{q}})\,, \quad (7)$$

$$\boldsymbol{\phi}(\mathbf{q}^d) = \mathbf{0}\,, \quad (8)$$

where $\mathbf{q}$ and $\mathbf{q}^d$ are the measured and the desired descriptor coordinates, respectively. Introducing $\mathbf{y}^d = \dot{\mathbf{q}}^d$, equations (7) and (8) can be rewritten as

$$\dot{\mathbf{q}}^d = \mathbf{y}^d\,, \quad (9)$$

$$\dot{\mathbf{y}}^d = \mathbf{M}^{-1}\Big(\mathbf{Q}_g + \mathbf{H}(\mathbf{q}^d)\mathbf{u} - \boldsymbol{\Phi}_{\mathbf{q}}^{\mathrm{T}}(\mathbf{q}^d)\boldsymbol{\lambda} - \mathbf{K}_P(\mathbf{q}^d - \mathbf{q}) - \mathbf{K}_D(\dot{\mathbf{q}}^d - \dot{\mathbf{q}})\Big), \quad (10)$$

$$\mathbf{0} = \boldsymbol{\phi}(\mathbf{q}^d)\,. \quad (11)$$

The set of equations (9–11) can be partitioned into the prescribed controlled coordinates and the uncontrolled coordinates yielding the vector of unknowns

$$\mathbf{z} = \left[\mathbf{q}_u^d \,,\, \mathbf{y}_u^d \,,\, \mathbf{u} \,,\, \boldsymbol{\lambda}\right]^{\mathrm{T}} \,. \tag{12}$$

Using the Backward Euler method, the set of difference equations $\mathbf{F}(\mathbf{z}) = \mathbf{0}$ has to be solved for the (n+1)*th* value of $\mathbf{z}$, where

$$\mathbf{F}_{n+1} = \begin{bmatrix} \mathbf{q}_{u,n+1}^d - \mathbf{q}_{u,n}^d - h\mathbf{y}_{u,n+1}^d \\ \mathbf{y}_{u,n+1}^d - \mathbf{y}_{u,n}^d - h\mathbf{f}_{n+1} \\ \mathbf{g}_{n+1} \\ \boldsymbol{\phi}_{n+1} \end{bmatrix} \quad \text{with} \tag{13}$$

$$\mathbf{f}_{n+1} = \mathbf{S}_u^{\mathrm{T}}\mathbf{M}^{-1}\big(\mathbf{Q}_g + \mathbf{H}(\mathbf{q}^d)\mathbf{u} - \boldsymbol{\Phi}_{\mathbf{q}}^{\mathrm{T}}(\mathbf{q}^d)\boldsymbol{\lambda} - \mathbf{K}_P(\mathbf{q}^d - \mathbf{q}) - \mathbf{K}_D(\dot{\mathbf{q}}^d - \dot{\mathbf{q}})\big) \,, \tag{14}$$

$$\mathbf{g}_{n+1} = -\dot{\mathbf{y}}_c^d + \mathbf{S}_c^{\mathrm{T}}\mathbf{M}^{-1}\big(\mathbf{Q}_g + \mathbf{H}(\mathbf{q}^d)\mathbf{u} - \boldsymbol{\Phi}_{\mathbf{q}}^{\mathrm{T}}(\mathbf{q}^d)\boldsymbol{\lambda} - \mathbf{K}_P(\mathbf{q}^d - \mathbf{q}) - \mathbf{K}_D(\dot{\mathbf{q}}^d - \dot{\mathbf{q}})\big) \,. \tag{15}$$

The solution of the above system can be obtained for the consecutive time steps with sampling time h, by iterating to $\mathbf{z}_{n+1}$ via the repeated solution of the equation

$$\mathbf{J}_{n+1}(\mathbf{z}_{n+1} - \mathbf{z}_n) = -\mathbf{F}_{n+1} \,, \tag{16}$$

where $\mathbf{J}$ is the Jacobian matrix

$$\mathbf{J} = \left[\begin{array}{c:c:c:c} \mathbf{I} & -h\mathbf{I} & \mathbf{0} & \mathbf{0} \\ \hdashline \begin{array}{l} h\mathbf{S}_u^{\mathrm{T}}\mathbf{M}^{-1}[\mathbf{K}_P\mathbf{S}_u + \\ (\boldsymbol{\Phi}_{\mathbf{q}}^{\mathrm{T}}\boldsymbol{\lambda})_{\mathbf{q}_u^d} - (\mathbf{H}\mathbf{u})_{\mathbf{q}_u^d}] \end{array} & \mathbf{I} + h\mathbf{S}_u^{\mathrm{T}}\mathbf{M}^{-1}\mathbf{K}_D\mathbf{S}_u & -h\mathbf{S}_u^{\mathrm{T}}\mathbf{M}^{-1}\mathbf{H} & h\mathbf{S}_u^{\mathrm{T}}\mathbf{M}^{-1}\boldsymbol{\Phi}_{\mathbf{q}}^{\mathrm{T}} \\ \hdashline \begin{array}{l} \mathbf{S}_c^{\mathrm{T}}\mathbf{M}^{-1}[\mathbf{K}_P\mathbf{S}_u + \\ (\boldsymbol{\Phi}_{\mathbf{q}}^{\mathrm{T}}\boldsymbol{\lambda})_{\mathbf{q}_u^d} - (\mathbf{H}\mathbf{u})_{\mathbf{q}_u^d}] \end{array} & \mathbf{S}_c^{\mathrm{T}}\mathbf{M}^{-1}\mathbf{K}_D\mathbf{S}_u & -\mathbf{S}_c^{\mathrm{T}}\mathbf{M}^{-1}\mathbf{H} & \mathbf{S}_c^{\mathrm{T}}\mathbf{M}^{-1}\boldsymbol{\Phi}_{\mathbf{q}}^{\mathrm{T}} \\ \hdashline \boldsymbol{\Phi}_{\mathbf{q}}\mathbf{S}_u & \mathbf{0} & \mathbf{0} & \mathbf{0} \end{array}\right] \tag{17}$$

with

$$(\boldsymbol{\Phi}_{\mathbf{q}}^{\mathrm{T}}\boldsymbol{\lambda})_{\mathbf{q}_u^d} = \frac{\partial \boldsymbol{\Phi}_{\mathbf{q}}^{\mathrm{T}}\boldsymbol{\lambda}}{\partial \mathbf{q}_u^d} \quad \text{and} \quad (\mathbf{H}\mathbf{u})_{\mathbf{q}_u^d} = \frac{\partial \mathbf{H}\mathbf{u}}{\partial \mathbf{q}_u^d} \,. \tag{18}$$

4 Real parameter case study and simulation

The planar ACROBOTER model was simulated with realistic mechanical and control parameters. The mass of the swinging unit was set to

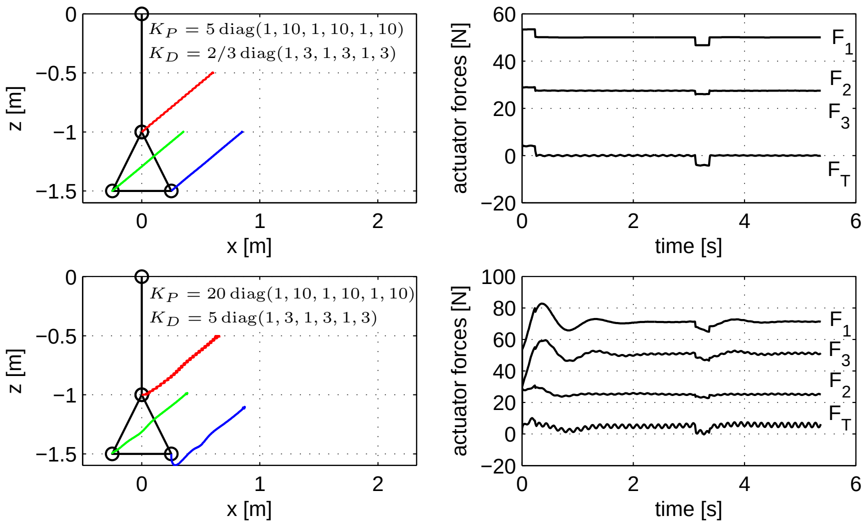

Figure 2. Simulation results

$m_{SU} = 5$kg, while the mass $m_{CC} = 0.1$kg was set relatively small compared to it. In addition, the geometry of the SU was given by the length of the rod $L_{34} = 0.5$m. As an important control parameter the sampling time of the system was $h = 10$ms during the simulation.

In the simulation the actuator forces were determined according to Section 3, while the equations of motion (1) and (2) were solved by using the method of Lagrange multipliers with Baumgarte stabilization (de Jalón and Bayo, 1994). This co-simulation made it possible to feed back the state of the system for the calculation of the actuator forces.

Figure 2 presents two sets of simulation results. In both cases the geometric center of the swinging unit was commanded to move along a straight line between the points (0, -1.5) and (0.6, -1). The trajectory had a trapezoidal velocity profile, characterized by the maximum acceleration and velocity $a_{max} = 1\mathrm{m/s}^2$ and $v_{max} = 0.25\mathrm{m/s}$, respectively. In the simulation presented in the top panels in Figure 2 the mass and inertia properties were considered as exactly known parameters of the system, i.e., the center of gravity and the geometric center were the same and the rod was considered to have homogeneous mass distribution. In contrast, the bottom panels show the simulation result when the effect of the payload were also considered. In this case, the mass of the SU was increased with a payload of 1kg. The payload was considered as a point mass causing the change of the common center of gravity expressed by $\rho_C = [0.3\mathrm{m}\,, -0.05\mathrm{m}]^{\mathrm{T}}$.

5 Conclusion

The computed torque control of an under-actuated service robot was presented. The calculation of the desired control inputs led to a DAE problem, which was solved via the Backward Euler discretization of the system and by using the Newton-Raphson method. The Jacobian matrix of the iteration algorithm was determined semi-analytically. The method is applicable for broad class of systems that can be modeled by natural coordinates.

The presented numerical results clearly show the applicability of the proposed control method. On the other hand, compensation is needed for modeling errors caused by unknown payloads. The tracking error can be decreased by increasing the values of the proportional gain matrix, while the stationary pose error at the final time may be eliminated by a PID controller. The limitations of the applied model based control may be improved by introducing an adaptation law for the control gains. Possible large disturbances are to be handled by the high level controller of the ACROBOTER, which may couple the separate controllers of the CU and SU.

Bibliography

C. Balaguer, A. Gimenez, A. J. Huete, A. M. Sabatini, M. Topping, and G. Bolmsjö. The MATS robot. *IEEE Robotics and Automation Magazine*, 13(1):51–58, 2006.

W. Blajer and K. Kolodziejczyk. Modeling of underactuated mechanical systems in partly specified motion. *Journal of Theoretical and Applied Mechanics*, 46 (2):383–394, 2008.

J.G. de Jalón and E. Bayo. *Kinematic and dynamic simulation of multibody systems: the real-time challenge*. Springer-Verlag, 1994.

J. Kövecses, J.-C. Piedoboeuf, and C. Lange. Dynamic modeling and simulation of constrained robotic systems. *IEEE/ASME Transactions on mechatronics*, 8(2):165–177, 2003.

I. M. M. Lammerts. *Adaptive Computed Reference Computed Torque Control*. PhD thesis, Eindhoven University of Technology, 1993.

FATEC Co. Walking assist system by supporting from ceiling (FLORA). http://www.fa-tec.co.jp/FLORA-C/index.htm, 2004. Last accessed: Dec. 2009.

T. Sato, R. Fukui, H. Mofushita, and T. Mori. Construction of ceiling adsorbed mobile robots platform utilizing permanent magnet inductive traction method. In *Proceedings of 2004 IEEEiRSJ International Conference on Intelligent Robots and Systems*, pages 552–558, 2004.

G. Stépán and et al. A ceiling based crawling, hoisting and swinging service robot platform. In *Proceedings of Beyond Gray Droids: Domestic Robot Design for the 21st Century Workshop at HCI 2009*, 2009.